

Supporting Information

Kilina et al. 10.1073/pnas.0711646105

SI Text

Computational Approach and (7,6) Tube Analysis. To study the excitonic structure in SWNTs, we used the following computational strategy. The initial structures of SWNTs were generated by using TubeGen 3.3 (1) and graphically visualized by XCrystal software (2). Optimal geometries were obtained by using the Austin Model 1 (AM1) semiempirical Hamiltonian (3) at the Hartree–Fock level using the MOPAC-2002 code (4). The AM1 approach was specifically designed for this purpose and was widely applied to calculate ground state (4, 5) properties of many molecular systems. The semiempirical approximation restricts the basis set to valence orbitals of Slater type, which limits the number of Hamiltonian matrix elements. Such a methodology makes semiempirical techniques significantly easier and faster, yet allows for an accurate description of a broad range of electronic phenomena. For example, no assumptions about the vibrational properties and curvature mediated σ and π interactions are necessary because the AM1 Hamiltonian has these effects built into the dependence of its matrix elements on the nuclei positions.

Optimized ground state geometries provide input structures for excited state calculations performed by using the Collective Electronic Oscillator (CEO) code combined with the Zerner's Intermediate Neglect of Differential Overlap (ZINDO) Hamiltonian (6, 7). ZINDO was developed specifically for calculating excited states and hence provides a better agreement with experimental electronic spectra. The CEO approach, described in detail elsewhere (e.g., in refs. 8 and 9), solves the equation of motion for the single-electron density matrix of a molecule driven by an external electric field using the TDHF approximation for the many-electron problem (10, 11). Numerically efficient Krylov space algorithms (e.g., Lanczos or Davidson) (8, 12, 13) make the expense of computation of excited states comparable to the ground state calculations.

Within this theoretical framework, the changes induced in the density matrix by an external field are expressed as linear combinations of the electronic transition densities $\{\xi_\eta\}$ (8, 9) defined as

$$(\xi_\eta)_{mn} = \langle \eta | c_m^\dagger c_n | g \rangle \quad [3]$$

and reflect the changes in the electronic density induced by an optical transition from the ground state $|g\rangle$ to an excited state $|\eta\rangle$. Here, c_m^\dagger (c_n) is the creation (annihilation) operator, and the indices m and n refer to the basis functions (e.g., atomic orbitals, AOs). The size and localization of an exciton center of mass with respect to the molecule alignment can be extracted from a two-dimensional real-space analysis (8, 9) of the calculated transition densities ξ_η (Eq. 3). The diagonal elements of the transition densities $(\xi_\eta)_{nn}$ represent the net charge induced in the n th AO by an external field. The off-diagonal elements $(\xi_\eta)_{mn}$ ($m \neq n$) represent the joint probability amplitude of finding an electron and a hole located on the m th and n th AO, respectively. We coarse-grain these values over the various orbitals that belong to each carbon atom. The hydrogen atoms are omitted because the terminal hydrogens participate weakly in the delocalized electronic excitations. For carbon atoms we use the following contraction: the total induced charge on each atom A is given by

$$(\xi_\eta)_A = \left| \sum_{n_A} (\xi_\eta)_{n_A n_A} \right|, \quad [4]$$

whereas an average over all off-diagonal matrix elements represents the effective electronic coherence between atoms A and B.

$$(\xi_\eta)_{AB} = \sqrt{\sum_{n_A m_B} [(\xi_\eta)_{n_A m_B}]^2}. \quad [5]$$

Here, the indices n_A and m_B run over all atomic orbitals localized on atoms A and B, respectively. The size of the resulting matrix $(\xi_\eta)_{AB}$ equals $N' \times N'$, with N' being the number of atoms in the molecule without hydrogens. Contour plots of $(\xi_\eta)_{AB}$ provide a unique footprint of the respective electronic transitions (8, 9) (see Fig. 1).

1. Frey JT, Doren DJ (2005) TubeGen 3.3 (Univ of Delaware, Newark).
2. Kokalj A (1999) Xcrysden—A new program for displaying crystalline structures and electron densities. *J Mol Graphics Modell* 17:176–179.
3. Dewar MJS, Zoebisch EG, Healy EF, Stewart JJP (1985) AM1: A new general purpose quantum mechanical molecular model. *J Am Chem Soc* 107:3902–3909.
4. Stewart F, P JJ (2000) MOPAC 2002 (Schrödinger, Inc, and Fujitsu, Ltd, Portland, OR), 972.01.
5. Franco I, Tretiak S (2004) Electron-vibrational dynamics of photoexcited polyfluorenes. *J Am Chem Soc* 126:12130–12140.
6. Zerner MC (1996) ZINDO, A semiempirical quantum chemistry program (Quantum Theory Project, Univ of Florida, Gainesville).
7. Baker JD, Zerner MC (1991) Characterization of the random phase approximation with the intermediate neglect of differential-overlap Hamiltonian for electronic spectroscopy. *J Phys Chem* 95:8614–8619.
8. Tretiak S, Mukamel S (2002) Density matrix analysis and simulation of electronic excitations in conjugated and aggregated molecules. *Chem Rev* 102:3171–3212.
9. Mukamel S, Tretiak S, Wagersreiter T, Chernyak V (1997) Electronic coherence and collective optical excitations of conjugated molecules. *Science* 277:781–787.
10. Thouless DJ (1972) *The Quantum Mechanics Of Many-Body Systems* (Academic, New York).
11. Ring P, Schuck P (1980) *The Nuclear Many-Body Problem* (Springer, New York).
12. Davidson ER (1975) Iterative calculation of a few of lowest eigenvalues and corresponding eigenvectors of large real-symmetric matrices. *J Comp Phys* 17:87–94.
13. Stratmann RE, Scuseria GE, Frisch MJ (1998) An efficient implementation of time-dependent density-functional theory for the calculation of excitation energies of large molecules. *J Chem Phys* 109:8218–8224.

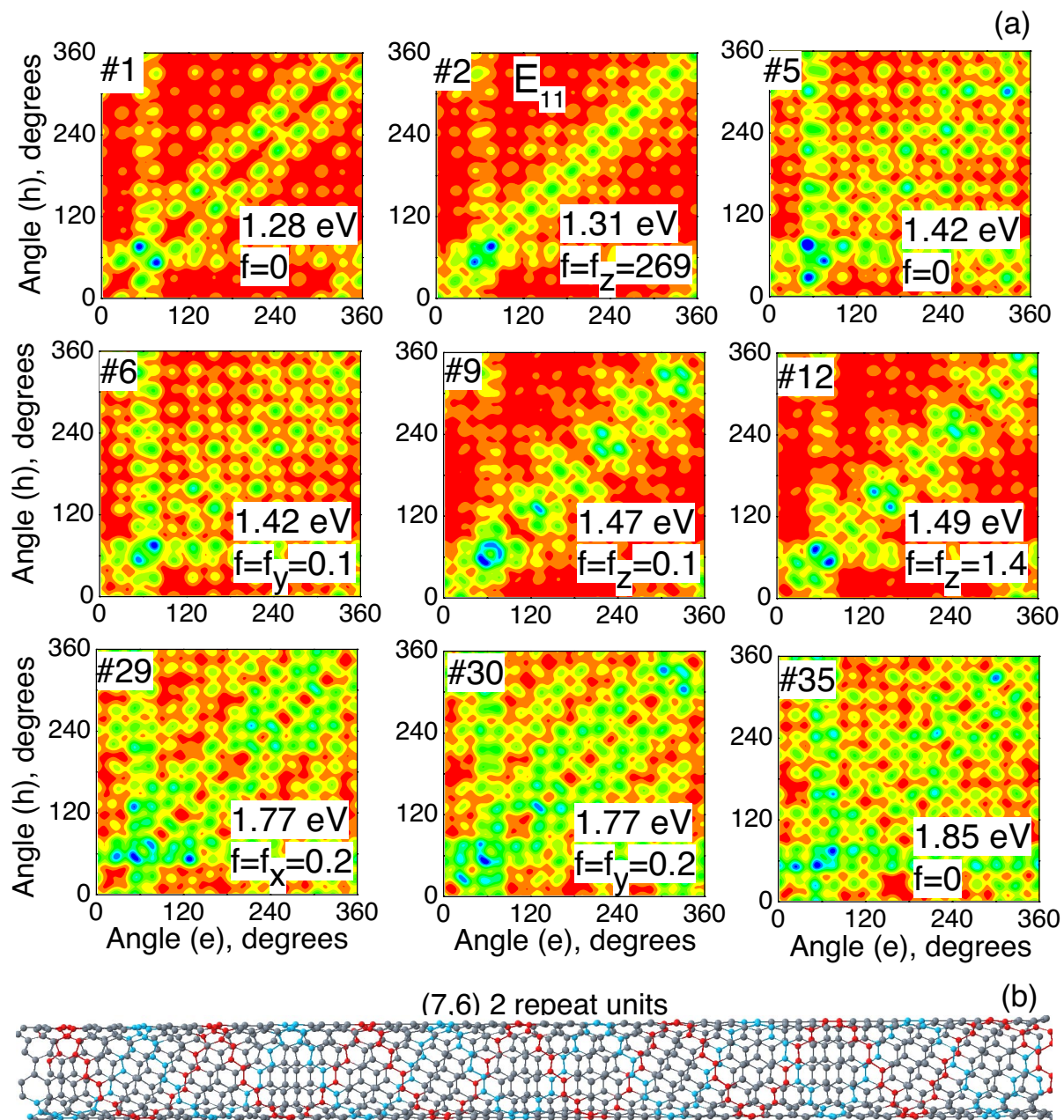


Fig. S1. (a) Contour plots of the transition density matrices corresponding to nine excitons of the (7,6) tube shown in the helical coordinate system schematically shown in b. Positions of the electron and hole are labeled with an azimuthal angle $0 < \phi_i < 2\pi$. The helical lines of the (7,6) tube are highlighted in red and cyan (orthogonal to the red line) on the tube surface. Four excitons labeled 1, 2 (bright state), 9, and 12 are attributed to parallel-polarized transitions because of their localized character with respect to the tube circumference. The other states are cross-polarized excitons.